Quaternary Research (2017), **88**, 446–457.

doi:10.1017/qua.2017.52

A multi-proxy lacustrine record of last deglacial–early Holocene environmental variability in the lower Yangtze region from the Chaohu Lake Basin, eastern China

Houchun Guan[a,b], Li Wu[c]*, Jinzhe Zhang[a], Shihao Shen[a], Dongru Chu[a], Linying Li[c]

[a]Geological Survey of Anhui Province, Hefei 230001, China
[b]School of Geographic and Oceanographic Sciences, Nanjing University, Nanjing 210023, China
[c]College of Territorial Resources and Tourism, Anhui Normal University, Wuhu 241002, China

(Received December 1, 2016; Accepted June 8, 2017)

Abstract

The Rb, Sr, and Ti content, Rb/Sr ratio, grain size, magnetic susceptibility, and magnetic fabric in sediments of the BZK1 core were utilized to reconstruct the evolution of the climatic environment in the Chaohu Lake Basin between the last deglacial and the early Holocene. Multi-proxy analyses indicate that lacustrine sediments in Chaohu Lake clearly record the Bølling-Allerød interstadial, the Younger Dryas event and dry-cold climate events occurring between 10.7 cal ka BP and 10.5 cal ka BP. At approximately 15.6–14.8 cal ka BP, the waters became deeper and the climate turned cool. The climate subsequently shifted to a relatively humid period and the lake was largest from 14.8 to 12.8 cal ka BP. From 12.8 to 11.7 cal ka BP, the climate abruptly turned dry and cold and the lake shrank to its lowest level. During 11.7–10.7 cal ka BP, the climate became relatively humid but, from approximately 10.7 to 10.5 cal ka BP, suddenly reverted to a dry and cold state. These climatic change records suggest that lacustrine sediments from the Chaohu Lake Basin in the lower Yangtze region responded actively to global climate changes, comparable with the environmental records from stalagmites and other lacustrine sediments in the region.

Keywords: Last deglacial; Early Holocene; Environmental variability; Lacustrine; Lower Yangtze region; Chaohu Lake; China

INTRODUCTION

Compared with the last interglacial period (Marine Isotope Stage [MIS] 5e), climatic conditions since the most recent deglacial (i.e., the transition out of the last glacial maximum) are more similar to the present (Lowe and Walker, 1997; Wang, 2011; Roberts, 2014), and since the study of past climatic instability of the Pleistocene/Holocene transition helps predict future trends, it has become a focus of research in recent years (Parrenin et al., 2013; Berke et al., 2014; Hong et al., 2014; Xiao et al., 2014; Sun and Feng, 2015; Winsor et al., 2015). The last deglacial in the northern hemisphere incorporated three relatively cold periods, namely the Oldest Dryas (15.1–14.7 ka BP), the Older Dryas (14.1–14.0 ka BP), and the Younger Dryas (12.9–11.7 ka BP), as well as two relatively warm periods, namely the Bølling (14.7–14.1 ka BP) and the Allerød (14.0–12.9 ka BP; Epstein, 1995; Stuiver et al., 1995; Alley and Clark, 1999; Friedrich et al., 2001; Shen et al., 2005; Veski et al., 2012; Kirby et al., 2013; Xiao et al., 2014).

The continuous record of lacustrine sediments is an important source of information on past climate change of the Pleistocene/Holocene transition period, and physical, chemical, biological, and other indicators of lacustrine sediments can effectively be used to reconstruct past precipitation and temperature changes (Fritz, 2008; An et al., 2010; Shen, 2009; Chen et al., 2010).

Fluviolacustrine deposits in the monsoon region of the Loess Plateau of China (Sun et al., 2007; Wu, 2009), alpine lake sediments in the southwest monsoon region (Xiao et al., 2014), and stalagmites in the middle and lower reaches of the Yangtze River at low latitudes of the southeast monsoon region (Wang et al., 2001, 2005), clearly record the unstable climatic events of the last deglacial. However, there are few reports on lacustrine sediments, which may record these same events in the lower Yangtze region, the southeast monsoon area of eastern China.

Chaohu Lake is a semi-enclosed lake in the lower Yangtze region, and is connected to the Yangtze River by the Yuxi River. The lake sediments record rich information on

*College of Territorial Resources and Tourism, Anhui Normal University, Wuhu 241002, China. E-mail address: jedi-wuli@163.com (L. Wu).

environment changes, with little human interference, between the last deglacial and the early Holocene (Chen et al., 2009; Dai et al., 2009; Wu et al., 2010, 2012; Luo et al., 2015; Li et al., 2017). Studies of the pollen, magnetic susceptibility, grain size, geochemistry, charcoal, and phytolith records of lacustrine sediments in the Chaohu Lake have focused on the Holocene (Wang et al., 2008; Wu et al., 2008; Chen et al., 2009; Dai et al., 2009; Hu et al., 2015; Luo et al., 2015). However, there is still little research on the period of the last deglacial and differences remain in the interpretation of the paleoclimatic significance of the magnetic susceptibility indicator, so that the nature of climate change during the last deglacial in the Chaohu Lake Basin is still unknown (Xie et al., 2006; Zhang et al., 2007; Wang et al., 2008). By studying core samples from the Chaohu Lake Basin in the lower Yangtze region, this research aims to reconstruct environmental variability between the last deglacial and the early Holocene based on multi-proxy lacustrine records, with accelerator mass spectrometry (AMS) ^{14}C dating control and high-resolution records of grain size, magnetic susceptibility, magnetic fabric, and elemental geochemistry. We discuss the response to global climate change recorded by lacustrine sediments in eastern China during this period, so as to understand the processes of environmental change and the responses of the Chaohu Lake Basin since the last deglacial.

MATERIALS AND METHODS

Regional setting and sampling

The Chaohu Lake, now with an area of about 770 km^2, covers a geographical range between 31°25′28″~31°43′28″N and 117°16′54″~117°51′46″E. It was formed on the river valley plain and developed in the late Pleistocene as a shallow water lake (Du et al. 2004; Chen et al., 2009). Mountains and hills between the Yangtze River and the Huai River surround the basin of the lake. The lake sediments are mainly derived from seven rivers, including the Hangbu, Fengle, Pai, Nanfei, Zhegao, Zhao, and Baishishan rivers, among which the Hangbu River provides the largest sediment content. The Yuxi River connects the lake to the Yangtze River (Fig. 1). The East Asian Summer Monsoon (EASM) dominates the current climate of the Chaohu Lake Basin, with precipitation mainly occurring from June to September. Annual rainfall is 1,000 mm and annual average temperature is 15.7°C. Rain and warm conditions occur in the same period; dry conditions usually occur with cool temperatures. As the geographical position of the basin is close to the boundary between the warm temperate zone and the northern subtropical monsoon zones of China, sediment records are sensitive to environmental changes in this area.

Lacustrine sediments deposited since the last deglacial are exposed on the western margins of Chaohu Lake and are mostly gray and grayish-black muddy clay and silt (Chen et al., 2009; Wu, 2010; Luo et al., 2015). Two single-acting GXY-1 engineering drills were used in sampling to obtain a core sample of 38.1 m from the BZK1 site No. 1 core of Beigongwei: (31°28′56″N, 117°13′33″E; site elevation: 7.96 m asl), in which the thickness of the Quaternary deposits was 35.8 m (Fig. 1). Based on AMS ^{14}C dating and regional comparison, multi-indicator sampling was only conducted for core depths of 562.5 to 740.0 cm (10,277–15,627 cal yr BP). The sampling interval was 5 cm. Five AMS ^{14}C samples and 35 samples of grain size, as well as anisotropy of magnetic susceptibility, Rb, Sr, and Ti, were collected. Due to the disturbance of the core, a sample of the 710 cm depth was not collected. Non-magnetic plastic boxes measuring 2 cm^3 were used to sample and indicate the direction of the top and bottom to test the anisotropy of magnetic susceptibility.

Sample analysis

AMS^{14}C dating was conducted in the Xi'an Accelerator Mass Spectrometry Center, Institute of Earth Environment, Chinese Academy of Sciences. Because there were no wood or plant materials found in the core samples of 562.5 cm to 740.0 cm deep, all the materials dated were bulk organics. Magnetic susceptibility and anisotropy of magnetic susceptibility were measured in the State Key Laboratory of Lithospheric Evolution with a KLY-3S Kappa Bridge magnetic susceptibility instrument (sensitivity: 2×10^{-8} SI) produced by the Czech AGICO company. Grain size was analyzed at Nanjing Normal University using a Mastersizer 2000 laser particle size analyzer, and then the grain size data were generated. Contents of Rb, Sr, and Ti were also measured by XRF at Nanjing Normal University.

RESULTS

Chronology

The five AMS ^{14}C dating results were calibrated by CALIB 7.0.2 (Reimer et al., 2013) and are shown in Table 1 and Figure 2. Linear fitting was conducted between corrected calendar age and core depth, according to the formula:

$$Y = 0.0318X + 233.45$$

In the formula, Y represents core depth (cm) and X represents calendar age (cal yr BP). The linear correlation coefficient R is 0.9836, showing a good correlation between age and depth, and also indicates the continuity of lacustrine sediments and the uniform sedimentation rate (i.e., 0.033 cm/yr) in this period (Fig. 1). The calendar age of each sample can be derived by piecewise interpolation. According to previous research (Zhang et al., 2007; Chen et al., 2009; Luo et al., 2015), there is little inorganic carbon in lacustrine sediments and the absence of carbonate rocks in this area indicate that the reservoir effect was minimal. Therefore, the lake reservoir effect can be neglected.

Grain size

The clay, silt, and sand content of sediments from the BZK1 drill hole of Chaohu Lake were assessed using the

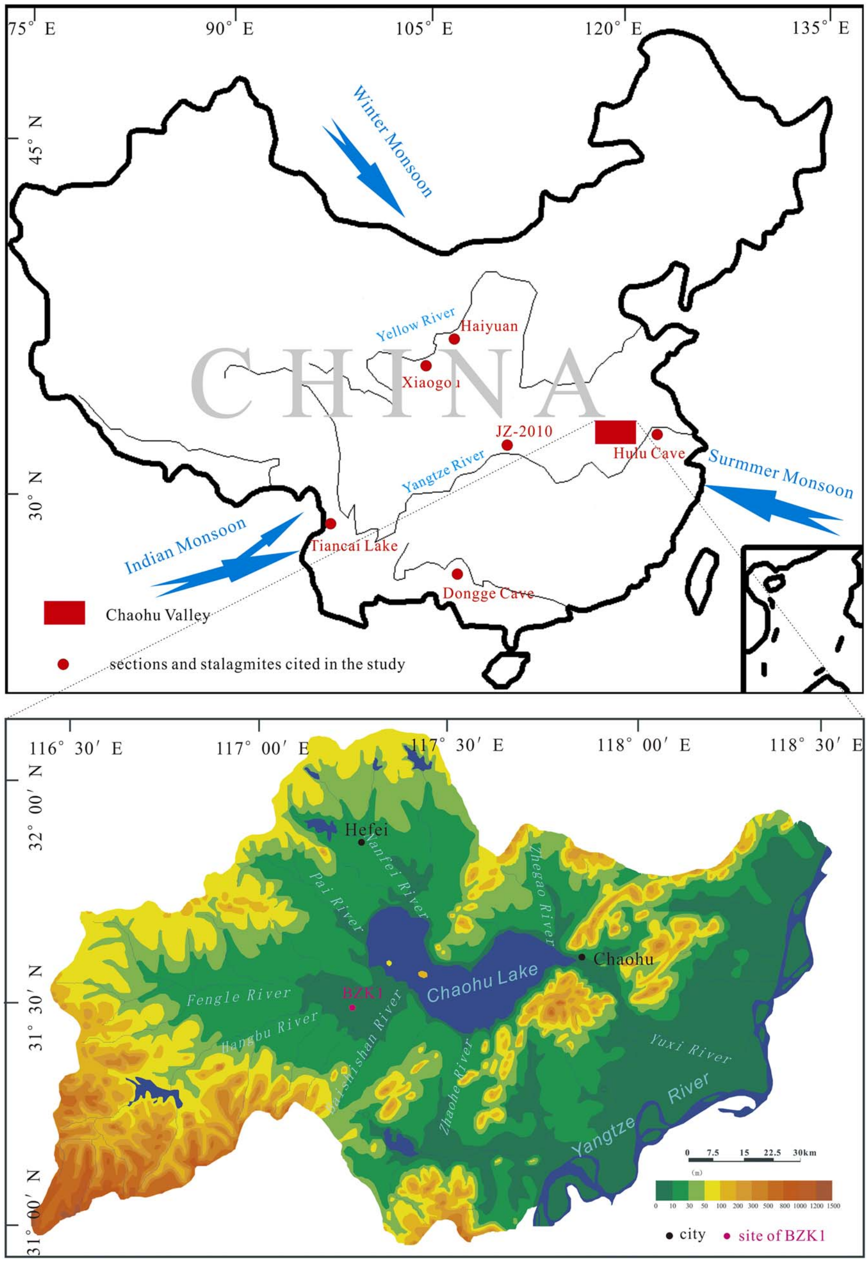

Figure 1. (color online) Location of BZK1 from Chaohu Lake Basin, Anhui Province, China and other sites mentioned.

Wentworth-Udden scale and the average grain diameters of sediments were calculated (Fig. 3).

Figure 3 shows that clay content was between 14.7 and 60.5%, with an average of 33.5%; silt content was between 39.5 and 82.3%, with an average of 65.2%; and sand content was between 0 and 4.7%, with an average of 1.2%. Silt comprises the majority of sediment, followed by clay, and sand content is very low. Figure 3 shows that the grain size of

Table 1. AMS^{14}C dating results and their calibrated ages of BZK1 from the Chaohu Lake Basin.

Sampling No.	Lab no.	Depth (cm)	AMS^{14}C age (yr BP)	Error (1σ)	1σ calibrated age	Calendar age (cal yr BP)
AMS ^{14}C-2	XA12017	562.5	9070	39	[10,209 cal yr BP: 10,245 cal yr BP] 1.00	10,227 ± 18
AMS ^{14}C-3	XA12016	595.0	9876	40	[11,231 cal yr BP: 11,293 cal yr BP] 0.914779	11,262 ± 31
AMS ^{14}C-4	XA12019	640.0	11743	47	[13,473 cal yr BP: 13,593 cal yr BP] 1.00	13,483 ± 60
AMS ^{14}C-5	XA12018	670.0	11872	45	[13,610 cal yr BP: 13,683 cal yr BP] 0.567745	13,647 ± 37
AMS ^{14}C-6	XA12020	740.0	13040	50	[15,505 cal yr BP: 15,749 cal yr BP] 1.00	15,627 ± 122

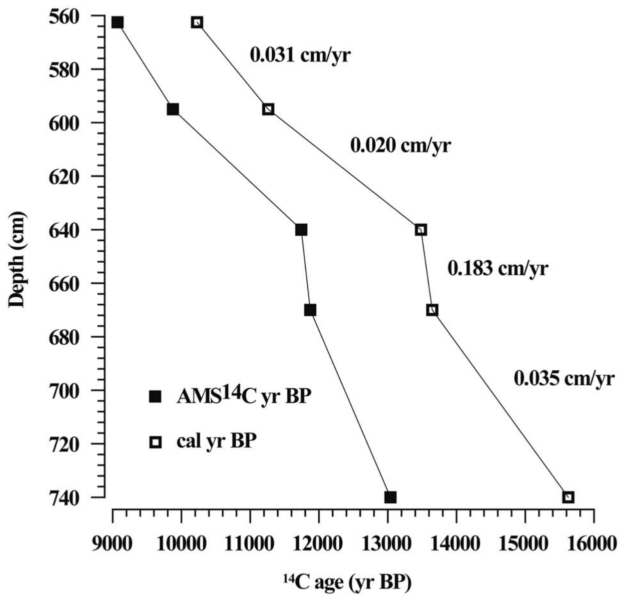

Figure 2. Accelerator mass spectrometry (AMS) ^{14}C dating ages of core BZK1 from the Chaohu Lake Basin.

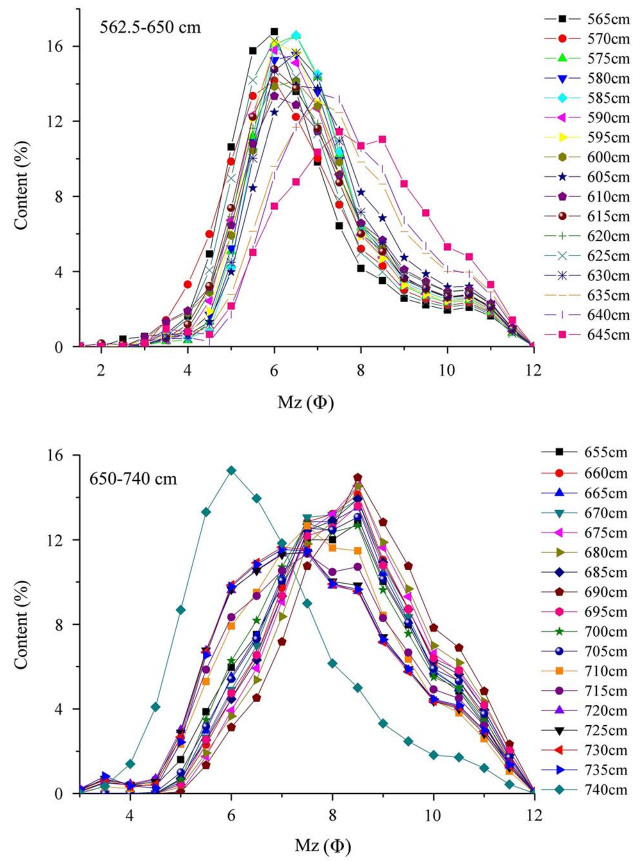

Figure 4. (color online) Frequency curves of core BZK1 from the Chaohu Lake Basin.

sediments differs between two sections, namely between the lower section from 645 to 740 cm and the upper section from 562.5 to 645 cm. In the lower section, clay content is between 16.0 and 60.5%, with an average of 44.2%; silt content is between 39.5 and 82.3%, with an average of 55.3%; sand content is between 0 and 1.75%, with an average of 0.5%, showing a significant increase in clay content, and silt and sand reduction in the entire core. In the upper section, clay content is between 14.7 and 41.6%, with an average of 22.3%; silt content is between 56.5 and 82.1%, with an average of 75.7%; and sand content is between 0.7 and 4.7%,

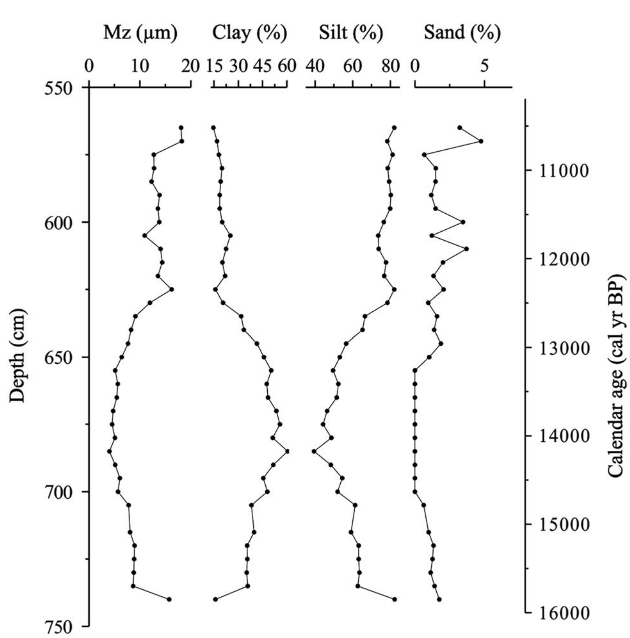

Figure 3. Variation of Mz, clay, sand, and depth of core BZK1 from the Chaohu Lake Basin.

with an average of 2.0%, showing significant increases in silt and sand content and a significant reduction in clay throughout the entire core. Figure 3 shows that the average grain diameter and variation of the sediment compositions are basically consistent with silt content. The grain size frequency distribution curves of the sediments also show that the mode of grain diameter of the part the core between 645 and 740 cm is between 3.9 and 2.0 μm and the mode of grain diameter of the part of the core between 562.5 and 645 cm is between 15.6 and 7.8 μm (Fig. 4). This feature is consistent with Figure 3, suggesting that suspended silt content is dominant in the lacustrine sediments.

Magnetic susceptibility and magnetic fabric characteristics

It can be seen from Figure 5 that the magnetic susceptibility and magnetic fabric of sediments differ between two sections, namely the lower from 645 to 740 cm and the upper from 562.5 to 645 cm. The magnetic susceptibility of the lower part ranges between 94.70×10^{-8} SI and 135.93×10^{-8} SI, with an average of 111.03×10^{-8} SI.

Figure 5 shows that the average F/L (magnetic foliation/magnetic lineation) value of the core section from 645 to 740 cm (15.6–13.0 cal ka BP) is 1.0021; the value

https://doi.org/10.1017/qua.2017.52 Published online by Cambridge University Press

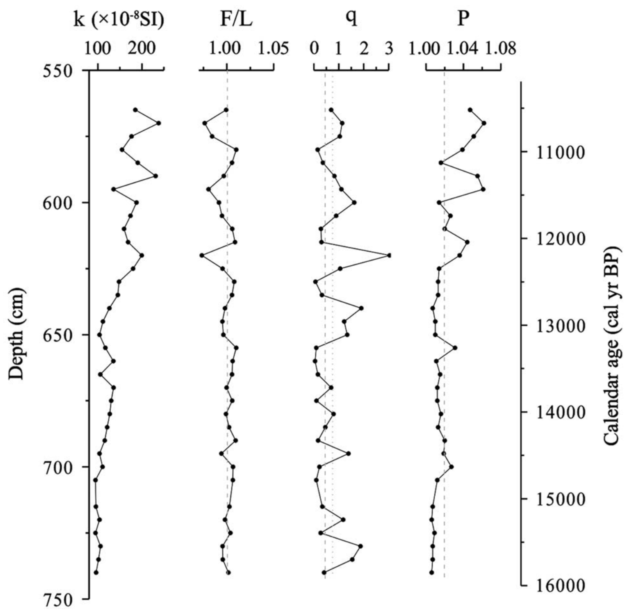

Figure 5. Variation of magnetic susceptibility and magnetic fabric along with depth of core BZK1 from the Chaohu Lake Basin.

of q (magnetic matrix particle size) is usually smaller than 0.5; and the average value of P (anisotropy of magnetic susceptibility) is 1.0133. The average F/L value of the core section from 562.5 to 645 cm (13.0–10.2 cal ka BP) is 0.9958; the value of q is usually greater than 0.5; and the average value of P is 1.0311 (P > 1.02).

Rb, Sr, and Ti characteristics

Figure 6 shows that Rb, Sr, Rb/Sr, and Ti values can also be divided into upper, middle, and lower segments with 645 and 705 cm as boundaries. In the lower segment, from 705 to 740 cm, Rb content ranges between 119.20 and 130.50 ppm, with an average of 126.20 ppm; Sr content ranges between 126.60 and 139.50 ppm, with an average of 134.13 ppm; the value of Rb/Sr ranges between 0.90 and 1.03, with an average of 0.94; and Ti content ranges between 4504.30 and 5030.80 ppm, with an average of 4808.30 ppm. In the middle segment, from 645 to 705 cm, Rb content ranges between 119.20 and 153.50 ppm, with an average of 142.11 ppm; Sr content ranges between 118.10 and 137.90 ppm, with an average of 126.53 ppm; the value of Rb/Sr ratio ranges between 0.88 and 1.29 with an average of 1.13; and Ti content ranges between 5046.50 ppm and 5783.60 ppm with an average of 5464.52 ppm. In the upper segment, from 562.5 cm to 645 cm, Rb content ranges between 94.60 and 115.30 ppm, with an average of 100.67 ppm; Sr content ranges between 129.20 and 155.90 ppm, with an average of 146.85 ppm; the value of Rb/Sr ranges between 0.88 and 1.29, with an average of 1.13; and Ti content ranges between 5046.50 and 5783.60 ppm, with an average of 5464.52 ppm.

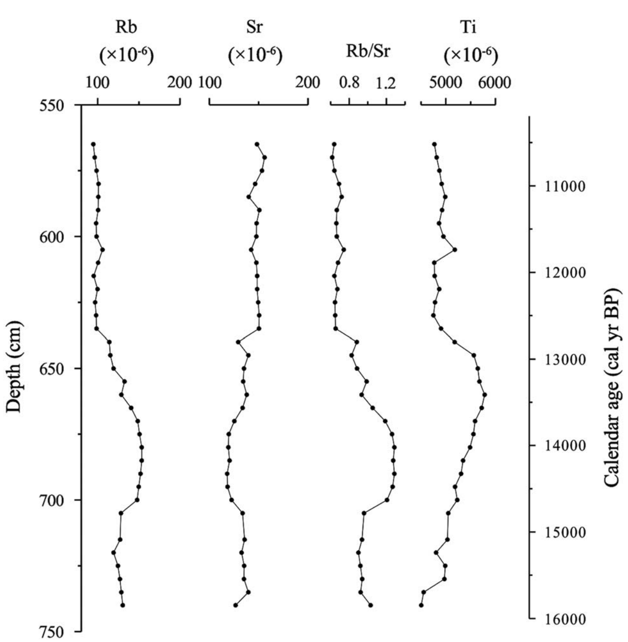

Figure 6. Variation of Rb, Sr, and Ti, and depth of core BZK1 from the Chaohu Lake Basin.

In short, the Rb and Sr content, and Rb/Sr values in the entire core are similar to the Rb value (between 76 and 223 ppm), Sr value (between 109 and 207 ppm) and Rb/Sr values (between 0.41 and 1.20) of the Xiashu Loess sections of the lower reaches of the Yangtze River (Li et al., 2003). Overall, Rb, Rb/Sr, and Ti feature relatively high values in the middle segment sandwiched between low values in the upper and lower segments. In contrast, Sr features relatively low values in the middle segment sandwiched between high values in the upper and lower parts.

DISCUSSION

Environmental significance of indicators

Grain size

The environmental significance of grain size in sediments is determined by the sedimentary environment (Finney and Johnson, 1991; Shi et al., 1999; Li et al., 2000; Sun et al., 2001; Chen et al., 2004; Shen, 2012). Overall, the sedimentary environment between 15.6 cal ka BP and 10.2 cal ka BP of the BZK1 core shifted from lacustrine sediments (15.6–13.0 cal ka BP) to lake margin and shoal sediments (13.0–10.2 cal ka BP). Considering the geographical location of the sampling site (Fig. 1), an increase in fine-grained sediments indicates an increase of lake volume and depth interpreted to indicate wetter conditions (Wang et al., 2008; Wu et al., 2010; Wang et al., 2012; Kirby et al., 2013). Similarly, an increase of coarse-grained sediments indicates drier conditions when the lake shrinks and waters are shallow (Wang et al., 2008; Wu et al., 2010; Wang et al., 2012; Kirby et al., 2013). It is also consistent with the evidence for water-level change of paleo-Gucheng Lake in the study region (Yao et al., 2007).

https://doi.org/10.1017/qua.2017.52 Published online by Cambridge University Press

Magnetic fabric and magnetic susceptibility

Magnetic fabric

Anisotropy of magnetic susceptibility (P) reflects the tendency of particle alignment in sediments, which is mainly controlled by sedimentary dynamics and environments. Generally, the stronger the sedimentary dynamics, and the more stable the sedimentary environments, the larger the value of P. Magnetic foliation (F) reflects the degree of surface distribution of sediment particles, which is the degree of fine bedding. The more development of fine bedding in the sediments, the larger the value of F, and vice versa. Magnetic lineation (L) reflects the extent of the long axis of the particles. Generally speaking, the more continuous and stable the fluid flow, the higher the value of L. Magnetic matrix particle size (q) is related to the uniformity of sediment particle size and the degree of particle arrangement. The more mixed the sediment particle size is, the higher the value of q is ($q > 0.7$).

Minima (maxima) in P, L (or L/F), q, and magnetic susceptibility (k) of sediment particles coincides with high (low) lake level, warm (cold, dry) periods, and retrogradation (progradation) of the lake (Wu et al., 1999; Yang and Li, 2000; Schneider et al., 2004; Zhang et al., 2004, 2008; Meissl et al., 2011; Yang et al., 2012). $F/L > 1$ and $q < 0.5$ show that the sedimentary environment is stable and magnetic foliation is more developed than magnetic lineation, indicating lacustrine sediments; $F/L < 1$ and $q > 0.7$ show that sedimentary environment is unstable and magnetic lineation is more developed than magnetic foliation, indicating fluvial and lakeshore deposits.

Figure 5 shows that values of F/L and q from the sediment in the core section from 645 to 740 cm (15.6–13.0 cal ka BP) range from 0.9940 to 1.0101 and 0.0454 to 1.8682, respectively, and are interpreted as indicating that the sedimentary environment was stable and lacustrine sediments were dominant, while values of F/L and q from the sediment in the core section from 562.5 to 645 cm (13.0–10.2 cal ka BP) range from 0.9732 to 1.0377 and 0.0613 to 3.0400, respectively, and indicate that lake fluctuations were large and lake margin sediments alternate with shoal sediments.

Magnetic susceptibility

Previous research has shown that grain size is an important factor affecting magnetic susceptibility, and that ferromagnetic ore in the tributary Hangbu River of Chaohu Lake Basin is the main magnetic mineral (Xie et al., 2006; Zhang et al., 2007). There are different relationships between magnetic susceptibility and grain size in the BZK1 core according to the change of sedimentary environments (Fig. 7). Sediments in the core section from 645 to 740 cm (15.6–13.0 cal ka BP) are interpreted as lacustrine sediments in which magnetic susceptibility negatively correlates with average grain diameter but positively correlates with clay content, and the sediments in this section are mainly fine particles, which are responsible for magnetic susceptibility. Increased magnetic susceptibility and decreases in particle diameter are interpreted to indicate humid climatic periods when the lake expanded and waters were deep, while the opposite indicate dry climatic periods when the lake shrank and waters were shallow.

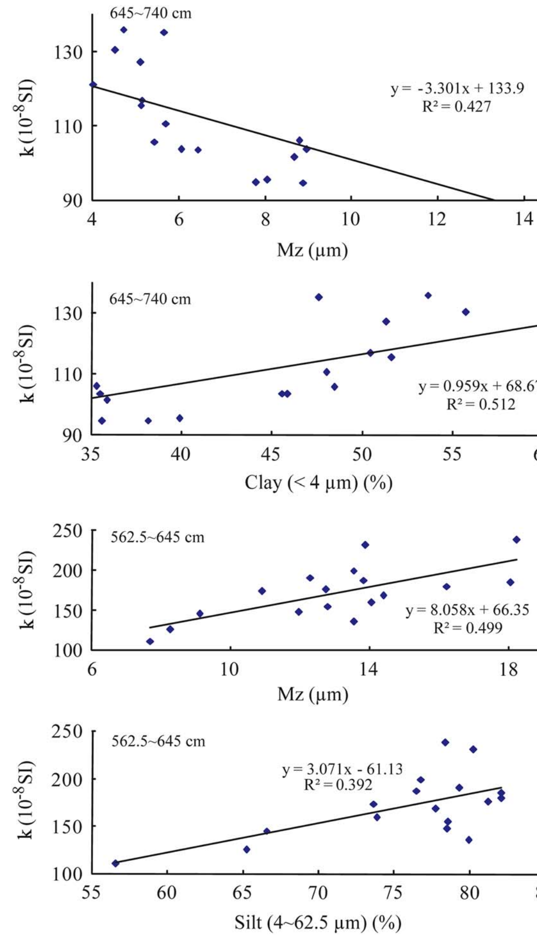

Figure 7. Relationship between magnetic susceptibility and grain size of core BZK1 from the Chaohu Lake Basin.

Sediments in the core section from 562.5 to 645 cm (13.0–10.2 cal ka BP) are lakeside and shoal sediments in which magnetic susceptibility positively correlates with average grain diameter and silt content. The sediments in this segment are mainly composed of silt, and the magnetic susceptibility of the sediments is mainly contributed by silt with coarse (sand-sized) particles. Figure 5 shows that the average magnetic susceptibility of the section from 562.5 to 645 cm, at 111.03×10^{-8} SI, is smaller overall than the average magnetic susceptibility of the section from 645 to 740 cm, which is 171.35×10^{-8} SI, showing that sediments with a high content of sand have a higher content of ferromagnetic ore, while sediments with a high content of clay have a lower content of ferromagnetic ore. Increases in both magnetic susceptibility and grain diameter are interpreted to indicate an arid climate in which the lake shrinks and waters are shallow; on the contrary, a decrease in grain diameter indicates a humid climatic period when the lake expands and waters are deep.

https://doi.org/10.1017/qua.2017.52 Published online by Cambridge University Press

Rb, Sr, and Ti

Rb has a large ionic radius and tends to exist in fine-grained clay during rock weathering and leaching, and its migration is very limited in weathering and pedogenic processes. However, the occurrence of the granular effect in Sr is more complex. Recent studies show that changes in Sr and Rb/Sr values are not only controlled by weathering, but also relate to the impact of sediment sources and grain size (Jin et al., 2002; Kalugin et al., 2005, 2007; Zeng et al., 2011; Li et al., 2012). The grain size distribution of authigenic minerals carrying Sr (such as carbonates) in lake sediments is different from that of Sr in terrigenous detrital minerals. When authigenic minerals predominate, Sr is mainly distributed in fine-grained sediments; when terrigenous detrital minerals predominate, Sr is mainly distributed in coarse-grained sediments. Non-residual Rb/Sr values mainly reflect the chemical weathering conditions of the basin, while residual Rb/Sr values mainly reflect the physical weathering conditions of the basin (Zeng et al., 2011). Enhanced summer monsoons, increased precipitation, increased intensity of surface runoff, enhanced runoff erosion, and increased deposition flux of terrigenous clast concentrate the stable element Ti in the surface sediments.

Comparison between Figure 3 and Figure 6 shows that Sr content changes with the average grain diameter of sediments, while Rb, Rb/Sr, and Ti negatively correlate with the average grain diameter (Mz). Based on the climatic conditions and geological background of Chaohu Lake, the environmental significance of Rb, Rb/Sr, and Ti in the region is: increases in Rb and Ti, decreases in Sr, and increases in Rb/Sr indicate that the grain size of sediments will be smaller if the EASM is enhanced, precipitation increases, and the water level of the lake rises; conversely, decreases in Rb, increases in Sr, and decreases in Rb/Sr indicate that the grain size of sediments will be greater if the summer monsoon is weakened, the climate is drier, and the water level of the lake drops. In other words, high Rb, Rb/Sr, and Ti with low Sr values indicate a humid climate caused by enhanced summer monsoon, while the opposite indicates a dry climate caused by a weakened summer monsoon.

Last deglacial–early Holocene climatic and sedimentary environment changes

Based on the variation of grain size, magnetic susceptibility, Rb, Sr, Ti, Rb/Sr, and other indicators, and considering the environmental background of the EASM region, changes in climatic environment between the last deglacial and the early Holocene in the Chaohu Lake Basin can be divided into five stages (Fig. 8):

Stage I (15.6–14.8 cal ka BP, 740–705 cm): k, with an average of 99.61×10^{-8} SI, and Ti, with an average of 4808 ppm, are interpreted to indicate that the climate in this stage was dry and cool. Among these indicators, grain size decreases, while magnetic susceptibility, Ti, and other values tend to increase, indicating that the lake gradually becomes deeper and the temperature fluctuates.

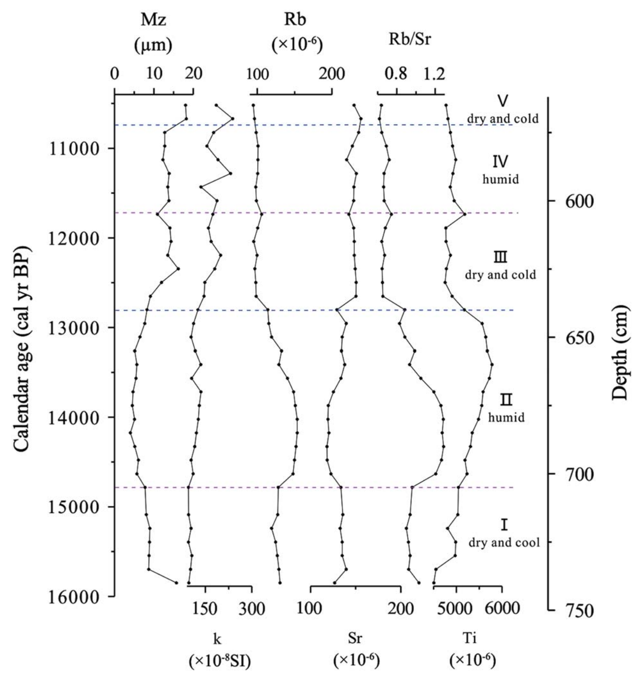

Figure 8. Multi-proxy records and comparison of core BZK1 from the Chaohu Lake Basin.

Stage II (14.8–12.8 cal ka BP, 705–640 cm): mean grain size with an average of 5.84 μm and Sr with an average of 127.64 ppm (units) are the lowest in the sequence. Rb/Sr ratio with, an average of 1.09, and Ti, with an average of 5451.14 ppm, are the highest in the five stages. k increases significantly compared with the former stage. All these indicate that there was a transition to a relatively humid climate during this stage and the lake at this point was at its largest during the last deglacial period.

Stage III (12.8–11.7 cal ka BP, 640–605 cm): there is a sharp increase in mean grain size. k tends to increase; Rb significantly decreases; Sr, with an average of 149.18 ppm, is relatively high; Rb/Sr, with an average of 0.66, is relatively low; Ti, with an average of 4807.73, ppm is also relatively low. All these indicate a sharp transition to a dry and cold climate during this stage when the lake shrank to its smallest dimensions during the last deglacial.

Stage IV (11.7–10.7 cal ka BP, 605–570 cm): mean grain size, with an average of 12.85 μm, and Sr, with an average of 146.93 ppm, decrease; Rb, with an average of 100.41 ppm, Rb/Sr, with an average of 0.68, and Ti, with an average of 4956.09 ppm, all increase. All these results indicate a transition to a relatively humid climate during this stage.

Stage V (10.7–10.5 cal ka BP, 570–565 cm): mean grain size sharply increases, and k and Sr increase. The values of Rb and Rb/Sr decrease and Ti also has a relative decrease. All the proxy indicators show that the climate during this stage became dry and cold again.

Regional comparison and response to global changes

The Bølling-Allerød warm periods

The climate in the Chaohu Lake Basin rapidly turned humid between 14.8 and 12.8 cal ka BP, which approximately coincides with the time interval of the Bølling-Allerød period (Stuiver et al., 1995; Alley and Clark, 1999; Friedrich et al., 2001; Veski et al., 2012; Xiao et al., 2014). The sediment record is consistent with the phytolith record from the lacustrine deposits of the Chaohu Lake (Luo et al., 2015). Comparisons can be made between this event and climatic instability recorded by stalagmites in the nearby Hulu Cave in Nanjing (Wang et al., 2001, 2005), fluvial-lacustrine sediments in mid-latitude plateau monsoon regions in southwest China (Sun et al., 2007; Wu, 2009), alpine lake sediments in low-latitude monsoon regions of China (Xiao et al., 2014), stalagmites in the Dongge Cave in Guizhou (Qin et al., 2004), deep-sea sediments (Bond et al., 1999), and the Greenland ice core (O'Brien et al., 1995; Fig. 9). Moreover, the variation in mean grain size, k, and Ti (Fig. 8) indicate that the Allerød period was wetter than the Bølling period according to the BZK1 core from Chaohu Lake Basin, which is similar to the records from the stalagmites in the Hulu Cave in Nanjing (eastern China; Wang et al., 2001); the Dongge Cave in Guizhou (southwestern China; Dykoski et al., 2005; Wang et al., 2005); and the Xiaogou section from Huining in Gansu and the pollen in the Haiyuan section from Ningxia (northwestern China; Sun et al., 2007; Wu, 2009). It is noteworthy that the character of changes in Rb, Sr, and Rb/Sr (Fig. 8) seems to be contrary to the above. This may result from local conditions such that, in the Bølling-Allerød period, the vegetation in the Chaohu valley area, located in the subtropical monsoon region, was well-developed. This impeded the physical removal of sediment so that non-residual Rb/Sr values are dominated by residual values, reflecting the physical weathering information of the basin. High Rb and Rb/Sr with low Sr values indicate a dry climate, while the opposite indicates a humid climate (Zeng et al., 2011). Therefore, Rb, Sr, and Rb/Sr variations (Fig. 8) indicate that the Allerød period was wetter than the Bølling period. This also shows that environmental significance of Rb, Sr, and Rb/Sr is complex and should be used in conjunction with other alternative indicators.

The Older Dryas event was not identified in this study. From the perspective of ice age calculation (Stuiver et al., 1995), the event only lasted for 80 years, but the temporal resolution of proxy indicators in this study was not sufficient, so further study based on higher resolution sampling should be conducted in the future.

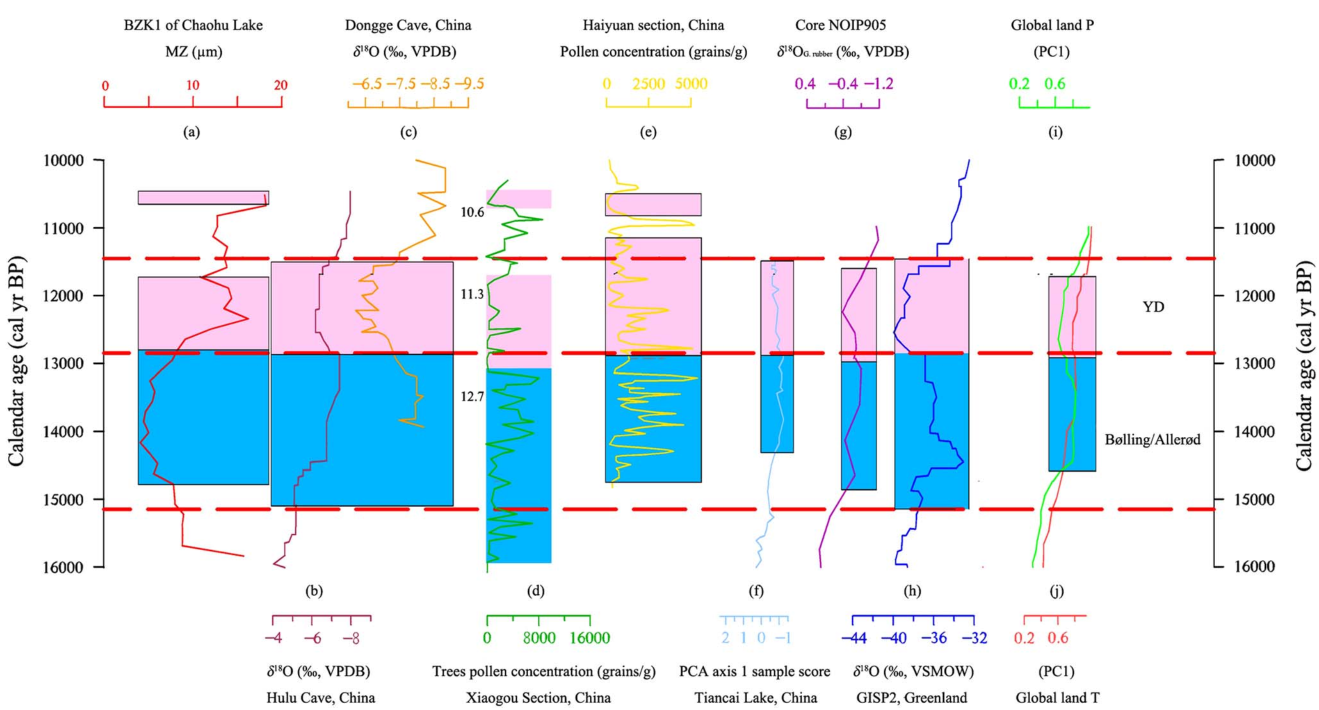

Figure 9. Regional and global correlations and forcing during the last deglaciation. (a) Mz from BZK1 of Chaohu Lake Basin before 10 cal ka BP in this study. (b) The oxygen isotope δ^{18}O (‰, VPDB) of Hulu Cave, China (Wang et al., 2001). (c) The oxygen isotope δ^{18}O (‰, VPDB) of Dongge Cave, China (Qin et al., 2004). (d) Tree pollen concentration (grains/g) in Xiaogou Section, China (Wu, 2009). (e) Pollen concentration (grains/g) in Haiyuan Section, China (Sun et al., 2007). (f) PCA (Principal Component Analysis) axis 1 sample score of pollen data in Tiancai Lake, China (Xiao et al., 2014). (g) The stable δ^{18}O record of the planktic foraminifera *G. ruber s.s.* for the NOIP905 core, western Arabian Sea (Huguet et al., 2006). (h) The oxygen isotope δ^{18}O (‰, VSMOW) from Greenland Ice Sheet Project Two (GISP2; Grootes and Stuiver, 1999). (i) Principal component (PC) 1 for precipitation in global land (green line) (Clark et al., 2012). (j) Principal component (PC) 1 for temperature in global land (red line). (For interpretation of the references to color in this figure legend, the reader is referred to the web version of this article.)

https://doi.org/10.1017/qua.2017.52 Published online by Cambridge University Press

The Younger Dryas event

During the period between 12.8 and 11.7 cal ka BP, there was a sharp transition to dry and cold conditions in the Chaohu Lake Basin, which can be compared with the Younger Dryas event (Stuiver et al., 1995; Bond et al., 1999). The phytolith record from the lacustrine deposits of the Chaohu Lake also suggested that the climate was cold and dry during 12.9–11.5 cal ka BP with unstable and low rainfall, which also corresponds to Younger Dryas event (Luo et al., 2015). The period is basically consistent with the start and end times of the Younger Dryas event recorded by stalagmites in the Hulu Cave in Nanjing (Wang et al., 2001) and the Dongge Cave in Guizhou (Qin et al., 2004), and can be compared with the Younger Dryas event recorded by the pollen from the Haiyuan section in Ningxia on the Loess Plateau (11.0–9.8 ka BP); the pollen from the Xiaogou section in Huining, the Zuli River Basin in central Gansu (10.7–9.9 ka BP); and the pollen from the alpine Tiancai Lake in northwestern Yunnan (12.9–11.5 ka BP) (Fig. 9). The above shows that the dry and cold event in this period, as recorded by Chaohu Lake Basin, is a response to global change.

The Early Holocene climate

Although the data in stage V are sparse, there are indications that the dry and cold climatic event can be compared with China's drought and sudden reduction of monsoon and rainfall in 10.2 ka BP (Wang et al., 2005); the drop in temperature in 10.9 ka BP based on stalagmite data from Yamen in Guizhou Province, China (Yang et al., 2010); the dry climate event of the section JZ-2010 of Jianghan Plain between 10.7 and 10.4 cal ka BP (Li et al., 2012); the remarkably dry and cold event in 10.6 cal ka BP recorded by the pollen from the Xiaogou section in Huining (Wu, 2009); the drop in temperature in 10.9 cal ka BP that is recorded by the pollen of Haiyuan section (Sun et al., 2007); the cooling event in 10.6 cal ka BP recorded in Okinawa, Japan (Xiang et al., 2007); the cold climate event in 10.3 ka BP that has been identified in ice-floating clastic samples of deep-sea sediments in the North Atlantic (Bond et al., 1997); and the weak Indian monsoon event in 10.2 ka BP recorded by Oman stalagmite from Socotra located in West Indian Ocean (Fleitmann et al., 2007; Fig. 9). The dry-cold event at 10.5 cal ka BP was also achieved from the color and magnetic susceptibility records of the lacustrine sediments in the Chaohu Lake (Hu et al., 2015). Most of these events lasted for a hundred years or so.

CONCLUSIONS

Our study has shown that: (1) the environmental significance of magnetic susceptibility differs between sedimentary environments in the BZK1 core of Chaohu Lake Basin. Between 15.6 and 13.0 cal ka BP, the sediments were lacustrine deposits; increases in magnetic susceptibility and decreases in grain diameter indicate a humid climatic period when the lake expanded and waters were deep. Between 13.0 and 10.2 cal ka BP, the sediments were lake shore and shoal deposits, in which increases in magnetic susceptibility indicate an arid climatic period when the lake shrank and waters were shallow. (2) The evolution of the climatic environment between the last deglacial and the early Holocene in the Chaohu Lake Basin is reconstructed as follows: between 15.6 and 14.8 cal ka BP, waters became deeper and the climate turned cool; between 14.8 and 12.8 cal ka BP, the climate shifted to relatively humid period and the lake was at its largest during the last deglacial; between 12.8 and 11.7 cal ka BP, the climate turned sharply dry and cold and the lake shrank to its smallest during the last deglacial; between 11.7 and 10.7 cal ka BP, the climate started to turn relatively humid; between 10.7 and 10.5 cal ka BP, the climate suddenly turned dry and cold. (3) The lacustrine sediments in Chaohu Lake clearly record the Bølling-Allerød interstadial, the Younger Dryas event, and dry-cold climate events occurring between 10.7 and 10.5 cal ka BP in the early Holocene, in contrast to records from stalagmites in Hulu Cave and low-latitude Dongge Cave, the pollens from Tiancai Lake and mid-latitude Haiyuan and Xiaogou, and the Greenland ice core, showing that climate changes recorded by the lacustrine sediments in eastern China responded actively to global changes.

ACKNOWLEDGMENTS

This work was supported by the National Natural Science Foundation of China (Grant No. 41401216), International S&T Cooperation Program of China (Grant No. 2014DFG91780), National Key Technologies R&D Program (2016YFA0600501), Land and Resources Survey Project from China Geological Survey Bureau (Grant Nos. 1212010610608, 12120113067800, 2016[041]-D32), Public Geological Survey Project of Anhui Province (Grant No. 2016-g-32). We are grateful to Zhongliang Chen and Jiayun Liu in Geological Survey of Anhui Province for their help in the field sampling, and Dr. Liang Yi and Dr. Huafeng Qin in the State Key Laboratory of Lithospheric Evolution for their help in the test. Special thanks to two reviewers, Prof. Xiaoping Yang and Dr Nicholas Lancaster for their valuable comments and suggestions that greatly improved this manuscript.

REFERENCES

Alley, R.B., Clark, P.U., 1999. The deglaciation of the northern hemisphere: a global perspective. *Annual Reviews of Earth and Planetary Sciences* 27, 149–182.

An, Z.S., Clemens, S.C., Shen, J., Qiang, X.K., Jin, Z.D., Sun, Y.B., Prell, W.L., et al., 2010. Glacial-interglacial Indian summer monsoon dynamics. *Science* 333, 719–723.

Berke, M.A., Johnson, T.C., Werne, J.P., Livingstone, D.A., Grice, K., Schouten, S., Damsté, J.S.S., 2014. Characterization of the last deglacial transition in tropical East Africa: Insights from Lake Albert. *Palaeogeography, Palaeoclimatology, Palaeoecology* 409, 1–8.

Bond, G., Showers, W., Cheseby, M., Lotti, R., Almasi, P., deMenocal, P., Priore, P., Cullen, H., Hajdas, I., Bonani, G., 1997. A pervasive millennial-scale cycle in north Atlantic Holocene and glacial climates. *Science* 278, 1257–1266.

Bond, G., Showers, W., Elliot, M., Evans, M., Lotti, R., Hajdas, I., Bonani, G., Johnson, S., 1999. The North Atlantic'S 1–2 ka climate rhythm: relation to Heinrich event Dansgarrd-Ochescher cycles and the Little Ice Age. *Geophysical Monograph* 112, 35–58.

Chen, F.H., Chen, J.H., Holmes, J., Boomer, I., Austin, P., Gates, J. B., Wang, N.L., Brooks, S.J., Zhang, J.W., 2010. Moisture changes over the last millennium in arid central Asia: a review, synthesis and comparison with monsoon region. *Quaternary Science Reviews* 29, 1055–1068.

Chen, J.A., Wan, G.J., Zhang, D.D., Zhang, F., Huang, R.G., 2004. Environmental records of lacustrine sediments in different time scales: sediment grain size as an example. *Science in China Series D Earth Sciences* 47, 954–960.

Chen, W., Wang, W.M., Dai, X.R., 2009. Holocene vegetation history with implications of human impact in the lake Chaohu area, Anhui Province, East China. *Vegetation History and Archaeobotany* 18, 137–146.

Clark, P.U., Shakun, J.D., Baker, P.A., Bartlein, P.J., Brewer, S., Brook, E., Carlson, A.E., et al., 2012. Global climate evolution during the last deglaciation. *Proceedings of National Academy of Sciences* 109, E1134–E1142.

Dai, X.R., Dearing, J.A., Yu, L.Z., Zhang, W.G., Shi, Y.X., Zhang, F.R., Gu, C.J., Boyle, J.F., Coulthard, T.J., Foster, G.C., 2009. The recent history of hydro-geomorphological processes in the upper Hangbu river system, Anhui Province, China. *Geomorphology* 106, 363–375.

Du, L., Yi, Z.L., Pan, S.M., 2004. Grain-size characteristics and sedimentary environment in the lacustrine deposit of Chaohu Lake, the Yangtze Delta region. [in Chinese with English abstract.] *Journal of Anhui Normal University (Natural Science)* 27, 101–104.

Dykoski, C.A., Edwards, R.L., Cheng, H., Yuan, D.X., Cai, Y.J., Zhang, M.L., Lin, Y.S., Qing, J.M., An, Z.S., Revenaugh, J., 2005. A high-resolution, absolute-dated Holocene and deglacial Asian monsoon record from Dongge Cave, China. *Earth and Planetary Science Letters* 233, 71–86.

Epstein, S., 1995. The isotopic climatic records in the Allerod-Boling-Younger Dryas and post-Younger Dryas events. *Global Biogeochemical Cycles* 9, 557–563.

Finney, B.P., Johnson, T.C., 1991. Sedimentation in Lake Malawi (East Africa) during the past 10 000 years: a continuous paleoclimatic record from the southern tropics. *Palaeogeography, Palaeoclimatology, Palaeoecology* 85, 351–366.

Fleitmann, D., Burns, S.J., Mangini, A., Mudelsee, M., Kramers, J., Villa, I., Neff, U., et al., 2007. Holocene ITCZ and Indian monsoon dynamics recorded in stalagmites from Oman and Yemen (Socotra). *Quaternary Science Reviews* 26, 170–188.

Friedrich, M., Kromer, B., Klaus, F., Kaiser, K.F., Spurk, M., Hughen, K.A., Johnsen, S.J., 2001. High-resolution climate signals in the Bolling/Allerod Interstadial (Greenland Interstadial 1) as reflected in European tree-ring chronologies compared to marine varves and ice-core records. *Quaternary Science Reviews* 20, 1223–1232.

Fritz, S.C., 2008. Deciphering climatic history from lake sediments. *Journal of Paleolimnology* 39, 5–16.

Grootes, P.M., Stuiver, M., 1999. GISP2 Oxygen Isotope Data. PANGAEA, doi: 10.1594/PANGAEA.56094.

Hong, B., Hong, Y.T., Uchida, M., Shibata, Y., Cai, C., Peng, H.J., Zhu, Y.X., Wang, Y., Yuan, L.G., 2014. Abrupt variations of Indian and East Asian summer monsoons during the last deglacial stadial and interstadial. *Quaternary Science Reviews* 97, 58–70.

Hu, F., Yang, Y.Z., Zhang, J.Z., Zheng, H.B., 2015. Sedimentary environmental evolution during Last Deglaciation and Early Holocene in Chaohu Region. [In Chinese with English abstract.] *Marine Geology and Quaternary Geology* 35(1), 153–162.

Huguet, C., Kim, J. H., Damsté, J.S.S., Schouten, S., 2006. Reconstruction of sea surface temperature variations in the Arabian Sea over the last 23 ka using organic proxies (TEX86 and UK′ 37). *Paleoceanography* 21, PA3003.

Jin, Z.D., Zhang, E.L., 2002. Paleoclimate implication of Rb/Sr rations from lake sediments. [In Chinese with English abstract.] *Science Technology and Engineering* 2, 20–22.

Kalugin, I., Daryin, A., Smolyaninova, L., Andreev, A., Diekmann, B., Khlystov, O., 2007. 800-yr-long records of annual air temperature and precipitation over southern Siberia inferred from Teletskoye Lake sediments. *Quaternary Research* 67, 400–410.

Kalugin, I., Selegei, V., Goldberg, E., Seret, G., 2005. Rhythmic fine-grained sediment deposition in Lake Teletskoye, Altai, Siberia, in relation to regional climate change. *Quaternary International* 136, 5–13.

Kirby, M.E., Feakins, S.J., Bonuso, N., Fantozzi, J.M., Hiner, C.A., 2013. Latest Pleistocene to Holocene hydroclimates from Lake Elsinore, California. *Quaternary Science Reviews* 76, 1–15.

Li, F., Wu, L., Zhu, C., Sun, W., Wang, X.C., Meng, H.P., Liu, H., et al., 2012. A High-resolution Study of Moisture Evolution in the Jianghan Plain Since 12.76 cal. ka B.P. [In Chinese with English abstract.] *Scientia Geographic Sinica* 32, 878–884.

Li, F.C., Xie, C.R., Jin, Z.D., Pan, G.X., 2003. Rubidium and strontium geochemistry in the Laohushan loess section, Nanjing, and relation between magnetic susceptibility and paleoclimatic change. [In Chinese with English abstract.] *Geology in China* 30, 93–98.

Li, J.Y., Dodson, J., Yan, H., Wang, W.M., Innes, J.B., Zong, Y.Q., Zhang, X.J., Xu, Q.H., Ni, J., Lu, F.Y., 2017. Quantitative Holocene climatic reconstructions for the lower Yangtze region of China. *Climate Dynamics*, doi: 10.1007/s00382-017-3664-3.

Li, Z.Z., Hai, Y., Luo, R.Y., Zhou, Y., Zhang, Q.J., 2000. Grain-size Characteristics and Sedimentary Environment in the Lacustrain Deposit of Downstream Area in Wulumuqi River Since 30 ka BP. [In Chinese with English abstract.] *Arid Zone Research* 17, 1–5.

Lowe, J.J., Walker, M.J.C., 1997. *Reconstructing Quaternary Environments.* 2nd ed. Routeledge, New York.

Luo, W.H., Zhang, J.Z., Yang, Y.Z., Yin, C.L., Shu, J.W., 2015. Late Pleistocene - middle Holocene environmental evolution: Phytolith record from the lacustrine deposits of the Chaohu Lake, Anhui. [In Chinese with English abstract.] *Acta Micropalaeontologica Sinica* 32, 63–74.

Meissl, S., Behrmann, J.H., Franke, C., 2011. Magnetic fabrics in Quaternary sediments, Ursa Basin, northern Gulf of Mexico record transport processes, compaction and submarine slumping. *Marine Geology* 286, 51–64.

O'Brien, S.R., Mayewski, P.A., Meeker, L.D., Meese, D.A., Twickler, M.S., Whitlow, S.I., 1995. Complexity of Holocene climate as reconstructed from a Greenland ice core. *Science* 270, 1962–1964.

Parrenin, F., Masson-Delmotte, V., Kohler, P., Raynaud, D., Paillard, D., Schwander, J., Barbante, C., Landais, A., Wegner, A., Jouzel, J., 2013. Synchronous change of atmospheric CO_2 and Antarctic temperature during the last deglacial warming. *Science* 339, 1060–1063.

Qin, J.M., Yuan, D.X., Cheng, H., Lin, Y.S., Zhang, M.L., Wang, H., Feng, Y.M., Tu, L.L., 2004. A high resolution late pleistocene climato-stratigraphy of 4 stalagmites from Qixing cave, Duyun, Guizhou. [In Chinese with English abstract.] *Quaternary Sciences* 24, 318–324.

Reimer, P.J., Bard, E., Bayliss, A., Beck, J.W., Blackwell, P.G., Ramsey, C.B., Buck, C.E., et al., 2013. IntCal13 and Marine13 radiocarbon age calibration curves 0–50,000 years cal BP. *Radiocarbon* 55, 1869–1887.

Roberts, N., 2014. *The Holocene: An Environmental History* (Third Edition). Wiley Blackwell, Chichester, UK.

Schneider, J. L., Pollet, N., Chapron, E., Wessels, M., Wassmer, P., 2004. Signature of Rhine Valley sturzstrom dam failures in Holocene sediments of Lake Constance, Germany. *Sedimentary Geology* 169, 75–91.

Shen, J., 2009. Progress and prospect of palaeolimnology research in China. [In Chinese with English abstract.] *Journal of Lake Sciences* 21, 307–313.

Shen, J., 2012. Spatiotemporal variations of Chinese lakes and their driving mechanisms since the Last Glacial Maximum: A review and synthesis of lacustrine sediment archives. *Chinese Science Bulletin* 58, 17–31.

Shen, J., Liu, X.Q., Wang, S.M., Ryo, M., 2005. Palaeoclimatic changes in the Qinghai Lake area during the last 18,000 years. *Quaternary International* 136, 131–140.

Shi, Q., Wang, J.M., Chen, F.H., 1999. Preliminary Study on Grain Size Characteristics of Sediments and Depositional Environment of Palaeo-terminal Lake of Shiyang River. [In Chinese with English abstract.] *Journal of Lanzhou University (Natural Sciences)* 35, 194–198.

Stuiver, M., Grootes, P.M., Braziunas, T.F., 1995. The GISP2 δ180 climate record of the past 1 6500 years and the roles of the sun, ocean and volcanoes. *Quaternary Research* 44, 341–354.

Sun, A.Z., Feng, Z.D., 2015. Climatic changes in the western part of the Chinese Loess Plateau during the Last Deglacial and the Holocene: a synthesis of pollen records. *Quaternary International* 372, 130–141.

Sun, A.Z., Ma, Y.Z., Feng, Z.D., Li, F., 2007. Pollen-recorded climate changes between 13.0 and 7.0 14C ka BP in southern Ningxia, China. *Chinese Science Bulletin* 52, 1080–1088.

Sun, Q.L., Zhou, J., Xiao, J.L., 2001. Grain-size characteristics of Lake Daihai sediments and its paleaoenvironment. [In Chinese with English abstract.] *Marine Geology and Quaternary Geology* 21, 93–95.

Veski, S., Amon, L., Heinsalu, A., Reitalu, T., Saarse, L., Stivrins, N., Vassiljev, J., 2012. Late glacial vegetation dynamics in the eastern Baltic region between 14,500 and 11,400 cal yr BP: A complete record since the Bølling (GI–1e) to the Holocene. *Quaternary Science Reviews* 40, 39–53.

Wang, S.W., 2011. *The Holocene Climate Change* [In Chinese.] China Meteorogical Press, Beijing.

Wang, X.C., Zhu, C., Wu, L., Sun, W., Li, F., Zhou, F.Q., Qi, S.Z., Gong, Q.L., 2012. Grain-size characteristics and sedimentary environment change of JZ-2010 section in Jianghan Plain, Hubei Province. [In Chinese with English abstract.] *Journal of Lake Sciences* 24, 480–486.

Wang, X.Y., Wu, L., Zhang, G.S., Wang, G.Y., Han, W.G., 2008. Characteristics and environmental significance of magnetic susceptibility and grain size of lake sediments since Holocene in Chaohu Lake, Anhui Province. [In Chinese with English abstract.] *Scientia Geographica Sinica* 28, 548–553.

Wang, Y., Cheng, H., Edwards, R.L., An, Z., Wu, J., Shen, C., Dorale, J.A., 2001. A high resolution absolute-dated late Pleistocene monsoon record from Hulu Cave, China. *Science* 294, 2345–2348.

Wang, Y.J., Cheng, H., Edwards, R. L., He, Y.Q., Kong, X.G., An, Z.S., Wu, J.Y., Kelly, M.J., Dykoski, C.A., Li, X.D., 2005. The Holocene Asian Monsoon: links to solar changes and North Atlantic climate. *Science* 308, 854–857.

Winsor, K., Carlson, A.E., Caffee, M.W., Rood, D.H., 2015. Rapid last-deglacial thinning and retreat of the marine-terminating southwestern Greenland ice sheet. *Earth and Planetary Science Letters* 426, 1–12.

Wu, H.B., Chen, F.H., Wang, J.M., Shi, Q., 1999. Study on magnetic fabric parameters of lake sediments in area and environmental changes. [In Chinese with English abstract.] *Marine Geology and Quaternary Geology* 19, 95–102.

Wu, H.L., 2009. *A high resolution record of vegetation and environmental variation through the last~25,000 years in the western part of the Chinese Loess Plateau* [In Chinese with English abstract.] Lanzhou University, Lanzhou.

Wu, L., Li, F., Zhu, C., Li, L., Li, B., 2012. Holocene environmental change and archaeology, Yangtze River Valley, China: Review and prospects. *Geoscience Frontiers* 3, 875–892.

Wu, L., Wang, X.Y., Zhang, G.S., Xiao, X.Y., 2008. Vegetation and climate evolution since the Holocene recorded by pollen-charcoal assemblages from lacustrine sediments of Chaohu Lake in Anhui Province. [In Chinese with English abstract.] *Journal of Palaeogeography* 10, 183–192.

Wu, L., Wang, X.Y., Zhou, K.S., Mo, D.W., Zhu, C., Gao, C., Zhang, G.S., Li, L., Liu, L., Han, W.G., 2010. Transmutation of ancient settlements and environmental changes between 6000–2000 aBP in the Chaohu Lake Basin, East China. *Journal of Geographical Sciences* 20, 687–700.

Xiang, R., Sun, Y.B., Li, T.G., Oppo, D.W., Chen, M.H., Zheng, F., 2007. Paleoenvironmental change in the middle Okinawa Trough since the last deglaciation: Evidence from the sedimentation rate and planktonic foraminiferal record. *Palaeogeography, Palaeoclimatology, Palaeoecology* 243, 378–393.

Xiao, X.Y., Haberle, S.G., Yang, X.D., Shen, J., Han, Y., Wang, S. M., 2014. New evidence on deglacial climatic variability from an alpine lacustrine record in northwestern Yunnan Province, southwestern China. *Palaeogeography, Palaeoclimatology, Palaeoecology* 406, 9–21.

Xie, H.X., Zhang, W.G., Gu, C.J., Dai, X.R., Yu, L.Z., John, D., 2006. Magnetic properties of sediments from Lake Chaohu and its response to sedimentary dynamics. [In Chinese with English Abstract.] *Journal of Lake Sciences* 18, 43–48.

Yang, X.Q., Li, H.M., 2000. Magnetic anisotropy and its environmental significance in continental faulted basin — taking the Nihewan Basin as an example. [In Chinese with English abstract.] *Marine Geology and Quaternary Geology* 20, 43–52.

Yang, X.Q., Su, Z.H., Yang, J., Huang, W.Y., 2012. Magnetic fabrics of Maar Lake sediments in tropical Southern China record hydrodynamic process. [In Chinese with English abstract.] *Quaternary Sciences* 32, 795–802.

Yang, Y., Yuan, D.X., Cheng, H., Zhang, M.L., Qin, J.M., Lin, Y.S., Zhu, X.Y., 2010. Precise dating of abrupt shifts in the Asian Monsoon during the last deglaciation based on stalagmite data from Yamen Cave, Guizhou Province, China. *Science China Earth Sciences* 53, 633–641.

Yao, S.C., Wang, X.L., Xue, B., 2007. Preliminary study of deposition pattern of Gucheng Lake at Jiangsu during Holocene.

[In Chinese with English abstract.] *Quaternary Science* 27, 365–370.
Zeng, Y., Chen, J.A., Zhu, Z.J., Li, J., 2011. Advance and porspective of Rb/Sr ratios in lake sediments as an index of Plaeoclimate/Paleoenvironment. [In Chinese with English abstract.] *Advances in Earth Science* 26, 805–810.
Zhang, W.G., Dai, X.R., Zhang, F.R., Shi, Y.X., Yu, L.Z., John, A.D., 2007. Magnetic properties of sediments from the Chaohu Lake for the last 7000 years and their implications for the evolution of Asian Monsoon. [In Chinese with English abstract.] *Quaternary Sciences* 27, 1053–1062.
Zhang, Y.F., Li, C.A., Chen, L., Kang, C.G., Yan, L.Q., Hu, S.H., Huo, J., 2008. Magnetic fabric of aqueous and aeolian sediments in the Middle Yangtze River. *Acta Geologica Sinica* 82, 857–863.
Zhang, Y.F., Li, C.A., Yan, G.L., Dong, X.H., 2004. A comparative study of magnetic fabric characters between flooded sediments and normal river sediments. [In Chinese with English abstract.] *Chinese Journal of Geophysics* 47, 639–645.